Cross-linker Mobility Governs Fracture Behavior of Catch-Bonded Networks

José Ruiz-Franco, Justin Tauber, and Jasper van der Gucht*
Physical Chemistry and Soft Matter, Wageningen University and Research, Stippeneng 4, 6708WE Wageningen, Netherlands

(Received 26 September 2022; accepted 24 January 2023; published 17 March 2023)

While most chemical bonds weaken under the action of mechanical force (called slip bond behavior), nature has developed bonds that do the opposite: their lifetime increases as force is applied. While such catch bonds have been studied quite extensively at the single molecule level and in adhesive contacts, recent work has shown that they are also abundantly present as crosslinkers in the actin cytoskeleton. However, their role and the mechanism by which they operate in these networks have remained unclear. Here, we present computer simulations that show how polymer networks crosslinked with either slip or catch bonds respond to mechanical stress. Our results reveal that catch bonding may be required to protect dynamic networks against fracture, in particular for mobile linkers that can diffuse freely after unbinding. While mobile slip bonds lead to networks that are very weak at high stresses, mobile catch bonds accumulate in high stress regions and thereby stabilize cracks, leading to a more ductile fracture behavior. This allows cells to combine structural adaptivity at low stresses with mechanical stability at high stresses.

DOI: 10.1103/PhysRevLett.130.118203

Many natural and engineering materials need to combine mechanical stability with structural adaptivity. Such seemingly contradictory properties can be realized in transient polymer networks: networks that are connected by dynamic, reversible bonds. The short-lived character of individual bonds allows for rearrangements and plasticity, while the mechanical integrity of the whole network can be maintained by distributing mechanical stresses over many bonds. This leads to viscoelastic behavior, and the possibility for stresses to relax and for damage to spontaneously heal [1]. Biological examples of transient networks can be found in the cytoskekeleton, where long actin filaments are linked together by a large variety of dynamic crosslinkers [2,3], and in the extracellular matrix, where protein fibrils and polysaccharides are crosslinked into a complex network by noncovalent interactions [4]. Synthetic examples of transient networks are associative polymers that carry hydrophobic sticky groups [5], hydrogen-bonding groups [6], or ionic interactions [7,8].

The mechanical stability of transient networks relies on a balance between bond breaking and reformation events. However, because forces acting on the linkers influence their binding and unbinding rates, this balance is shifted by mechanical stress. Local unbinding events can lead to small defects or microcracks in the material, which tend to concentrate stresses. Most crosslinkers unbind faster when force is applied, so that bond rupture is enhanced near defects, destabilizing these regions even further. This cascade of force-induced bond rupture ultimately leads to crack initiation and fracture, thereby compromising the resistance of transient networks against mechanical stress [1,9].

Recent findings suggest that nature may have found a way to avoid this catastrophic cascade of bond disruption, by making use of so-called catch bonds. Instead of weakening under force (called slip bond behavior), catch bonds first become stronger when they are stressed and weaken only at higher forces [see Fig. 1(a)]. This counterintuitive behavior emerges from a conformational rearrangement within the molecule upon the application of a mechanical force. First discovered in adhesion proteins [10–14], catch bonding has recently also been demonstrated in several crosslinking proteins in the cytoskeleton [15–19]. Since catch bonds become more stable at moderate forces, they may be able to stabilize networks against fracture by accumulating in regions of high stress, and thereby mitigate the vulnerability of transient networks to defects and cracks.

As suggested by recent simulations, the mechanical stability of transient networks depends sensitively on the mobility of the crosslinkers. Mobile linkers, such as actin-binding proteins that can diffuse freely after unbinding, can rebind in new locations of the network, and so redistribute rapidly. Immobile crosslinkers, however, such as pendant sticky groups attached to the polymer backbone, can only rebind in the same location. For slip bonds, crosslinker mobility is expected to accelerate fracture, because dissociated bonds can diffuse away from the crack tip and rebind in regions of lower stress [20]. By contrast, mobile catch bonds may be able to stabilize networks more efficiently than immobile catch bonds, because they can accumulate in regions of high stress [18].

To test this hypothesized stabilization mechanism of catch bonds, we perform computer simulations for networks with mobile and immobile slip bonds. Biological polymer networks are highly disordered and heterogeneous, which leads to very heterogeneous stress distributions and strongly

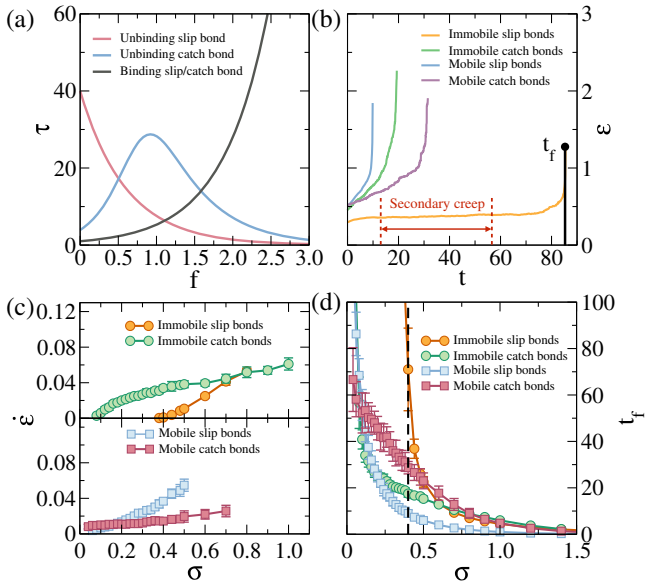

FIG. 1. (a) Unbinding times $\tau_u = 1/k_u$ and binding times $\tau_b = 1/k_b$ for slip and catch bonds. (b) Strain as a function of time for the four different types of crosslinkers, for $\sigma = 0.40$. The secondary creep phase and the network lifetime t_f are indicated for the immobile slip bond simulations. (c) Secondary creep rate and (d) lifetime of the network before fracture as a function of σ for the four networks simulated here. The vertical dashed line indicates the onset of metastability for the immobile slip bonds, for which no fracture was observed during our simulations.

nonaffine deformation fields [21–26]. We therefore use a network model in which the connectivity and topology are explicitly accounted for and in which nonaffine deformations and inhomogeneous stresses arise naturally. We consider a 2D network consisting of $L \times L$ nodes that can be connected by linear Hookean springs with the force-extension relation $f = \mu(l - l_0)/l_0$. We set the stiffness μ and rest length l_0 to unity for all springs, so that all forces are expressed in units of μ and all length scales in units of l_0. The transient nature of the network is accounted for by allowing bonds between nodes to bind and unbind stochastically, using a kinetic Monte Carlo scheme (KMC) [27]. Slip bond behavior is described using Bell's model, which assumes an exponential increase of the unbinding rate k_u with force [28], while catch bond behavior is described using the two-pathway model [29,30]. As natural catch bonds tend to be weaker than slip bonds [18], we choose parameters for which the lifetime of catch bonds at rest is much shorter than for slip bonds, as shown in Fig. 1(a), which shows the bond lifetimes $\tau_u = 1/k_u$ as a function of force for both types. We furthermore assume that the rebinding rate k_b decreases with increasing distance between the nodes, and take this to be the same for both types of bonds, as also shown in Fig. 1(a). All times are expressed in units of the binding time at zero force, $1/k_0^b$. To study how linker diffusion affects the mechanics of the network, we compare mobile and immobile bonds. While the binding and unbinding of immobile bonds always involve the same pair of nodes, mobile bonds are allowed to rebind at any location in the network, which corresponds to the limit of rapid diffusion after unbinding. To enable mobile bonds to redistribute, we allow the formation of double bonds. However, the number of actually bound linkers $N_b(t)$ can never exceed the total number of linkers N, which we take to be equal to the number of bonds in a network that is fully connected by single bonds. To study network failure under mechanical loading, we subject the networks to uniaxial deformation by applying a constant macroscopic stress $\sigma_{yy} \equiv \sigma$ at the top and bottom boundaries, while we use periodic boundary conditions in the x direction. We assume that the network is athermal, and use the FIRE algorithm to minimize the potential energy after every binding or unbinding event, by adjusting the positions of the nodes in the network [31]. While our model ignores the contribution of thermal fluctuations to the mechanical response, it has been shown previously that 2D athermal network models give a very good description of biological networks of semiflexible fibrils [32]. In all cases, we start with a fully (single-)connected triangular network and perform an equilibration process during 10^5 KMC steps at $\sigma = 0$, before applying the deformation. A detailed description of the model is presented in the Supplemental Material [33]. All quantities reported are averaged over 25 independent configurations for each stress.

Throughout this Letter, we will compare networks with four different types of crosslinkers: immobile and mobile slip bonds, and immobile and mobile catch bonds. In Fig. 1(b) we show how the four different networks deform after applying stress ($\sigma = 0.40$), by plotting the macroscopic strain ε as a function of time t. In all cases, we observe an initial elastic response, followed by a stage in which the strain grows more or less linearly (denoted secondary creep), until it finally fractures. We compute the creep rate $\dot{\varepsilon}$ in the secondary creep stage and the time to fracture t_f, and plot these as a function of σ in Figs. 1(c) and 1(d). We first discuss the case of immobile bonds. Clearly, the creep rate is much larger for immobile catch bonds than for immobile slip bonds. This is a consequence of the larger intrinsic unbinding rate k_0^u of catch bonds compared with slip bonds, making catch-bonded networks more dynamic. While the creep rate increases almost linearly with increasing stress for slip bonds, it levels off at intermediate stresses for catch bonds. We can further interpret these data by calculating the effective creep viscosity as $\eta = \sigma/\dot{\varepsilon}$. As shown in Fig. S1 in the Supplemental Material [33], the force-enhanced unbinding kinetics for slip bonds gives rise to strain thinning behavior (i.e., a viscosity that decreases with increasing stress), while for catch bonds, the strain thinning behavior at small forces is followed by strengthening of bound linkers at larger forces, giving rise to strain thickening. When considering the network lifetime t_f, we find that for all stresses, immobile slip bonds are more efficient in postponing

fracture than immobile catch bonds. In particular, for slip bonds we find a metastable region for $\sigma \lesssim 0.40$ [highlighted by the dashed line in Fig. 1(d)], for which no fracture is observed during our simulations and the creep rate vanishes. This metastable state shifts to much lower stresses for catch bonds. These findings show that, although immobile catch bonds can qualitatively change the response of the network to stress, they are not very efficient in protecting networks against fracture.

The picture changes dramatically, however, when the bonds are mobile, so that they can redistribute within the network. As shown in Fig. 1(c), crosslinker mobility strongly enhances the creep rate for slip-bonded networks. This enhanced creep significantly accelerates fracture, and removes the metastable regime that was observed for immobile slip bonds [Fig. 1(d)]. Such an adverse effect of mobility on the stability of slip-bonded materials was also observed in 1D simulations of adhesive patches [20]. Interestingly, for catch bonds mobility has the opposite effect: it reduces the rate of creep and delays fracture. Catch bonding thus provides a mechanism to stabilize networks with dynamic, diffusable linkers, such as those in the cytoskeleton. In particular, mobile catch bonds can combine deformability and adaptivity at low stresses (note that for $\sigma \lesssim 0.10$ the creep rate significantly exceeds that of slip bond networks), with rigidification and stabilization at higher stresses. These findings are in good agreement with experimental studies on actin networks crosslinked with α-actinin: networks crosslinked with the wild type protein, that shows catch bond behavior, had a much higher resistance to fracture than networks crosslinked with a slip-bonding mutant [18]. Moreover, while the slip bond variant led to stress softening networks, the catch bond wild type gave rise to shear thickening and stress-induced gelation [17,34], in accordance with our simulation results.

To obtain microscopic insight into the underlying crosslinker dynamics, we consider the evolution of the number of bonds in the network n_b as a function of time. For immobile slip bonds, shown in Fig. 2(a), n_b decays gradually after applying stress, and, as expected based on the lifetime-force relation of the bonds, this decay is faster when the stress increases. The metastable state for low stresses corresponds to a plateau in n_b [gray curve in Fig. 2(a)], in which bond rupture is balanced by rebinding, so that small cracks can be repaired before they start to propagate. For immobile catch bonds, the decay rate is less dependent on the stress [Fig. 2(b)]. While this shows that the catch mechanism is indeed activated in these networks, it does not lead to a longer network lifetime [Fig. 1(d)]. The scenario changes for the case of mobile bonds. As shown in the upper panels of Figs. 2(c) and 2(d), the number of single bonds decreases similarly as for immobile bonds. However, this decrease is now accompanied by an increase in the number of double bonds (shown in the lower panels). This increase of $n_{b,2}$ indicates that the dissociated bonds rebind

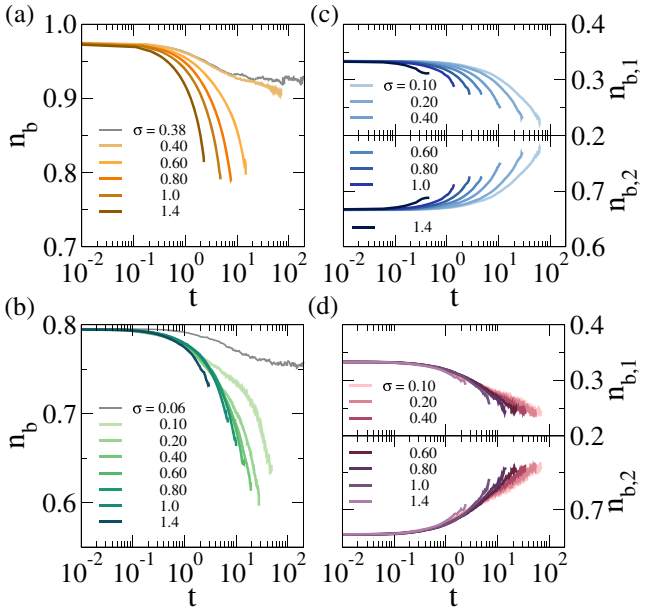

FIG. 2. Evolution of the normalized number of bonds in the network for different stresses σ, shown as $n_b = N_b(t)/N$ with $N_b(t)$ the number of bonds present at time t and N the maximum number of bonds, for (a) immobile slip bonds, (b) immobile catch bonds, (c) mobile slip bonds, and (d) mobile catch bonds. For the mobile bonds, the evolution of single bonds $n_{b,1}$ and double bonds $n_{b,2}$ is shown separately.

in other regions of the network. The total number of bonds, $n_{b,1} + n_{b,2}$, remains more or less constant (Fig. S3 in the Supplemental Material [33]), but their distribution over the network is strongly affected by the applied stress. For slip bonds, this bond redistribution destabilizes the network, in particular for higher stresses, since the network ruptures already after a small change in $n_{b,1}$ and $n_{b,2}$. For catch bonds, however, this is not so, indicating that the new bonds are placed in regions where they stabilize the network, i.e., in regions where the stress is higher. This can also be seen by looking at the probability distribution of the forces at which the bonds break and reform, shown in Fig. S5 in the Supplemental Material [33]. While the distribution for rebinding is very similar for the two different bonds, slip bonds that are more stretched break much more rapidly than stretched catch bonds.

Next, we study how the binding and unbinding events affect the evolution of the structure of the network. Representative snapshots of the networks just before macroscopic fracture are shown in Figs. 3(a)–3(d) for the four different crosslinkers at $\sigma = 0.40$. The evolution of these networks in time is shown in Figs. S11 and S12 in the Supplemental Material [33], where we see the formation of cracks that open up due to the applied tensile force. We calculate the distribution of crack sizes $P(c)$ from these snapshots. As explained in the Supplemental Material [33], cracks are identified by first mapping all bonds onto

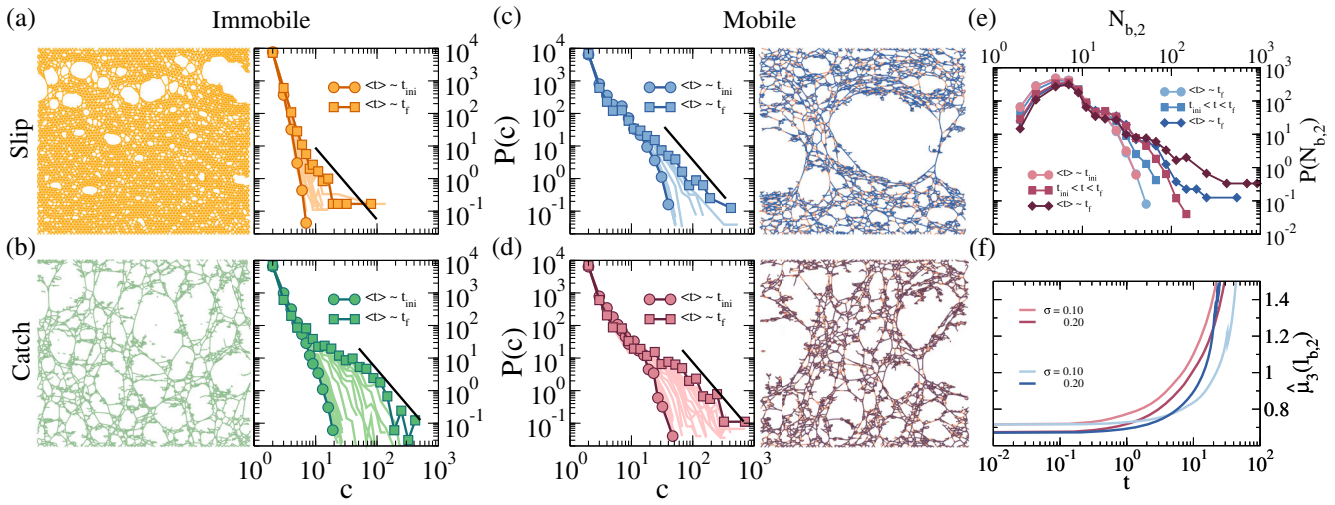

FIG. 3. Snapshots of the networks just before macroscopic fracture, and the evolution of the crack size distribution $P(c)$ at stress $\sigma = 0.40$ for (a) immobile slip bonds, (b) immobile catch bonds, (c) mobile slip bonds, and (d) mobile catch bonds. For networks with mobile bonds, the orange color corresponds to single bonds, while blue and purple indicate double slip and catch bonds, respectively. In each panel, a slope of -2.2 is indicated. The initial and final $P(c)$ are indicated by circles and squares, respectively, and the intermediate times are shown as drawn lines. (e) Distribution of double bonds located at the crack surface, and (f) skewness $\hat{\mu}_3$ of the double bond length distribution $l_{b,2}$ for networks with slip bonds (blue) and catch bonds (red), for different values of σ.

the original, undeformed triangular mesh, and then connecting centroid points of triangular cells that are no longer separated by a bond [33]. The results are shown in Fig. 3 next to the snapshots. Both the snapshots and the crack size distributions reveal different fracture scenarios for slip and catch bonds. For networks with slip bonds, the crack size distribution remains narrow, and the damage is localized in a few large cracks that will eventually merge, leading to macroscopic failure [Figs. 3(a) and 3(c)]. For catch bonds, $P(c)$ is much wider, and it develops a power law tail with an exponent $\alpha = -2.2$, which is close to the value expected for random percolation [35]. These findings suggest that the fracture evolution proceeds in a different manner for the different types of bonds. For slip bonds, stress concentration destabilizes especially the larger cracks, because the stress is largest at the tip of the largest cracks [36], and, as a consequence, the rupture rate is highest there. This leads to a scenario of crack nucleation and propagation. By contrast, catch bonds stabilize these high stress regions, and thereby prevent crack propagation. This leads to a broader crack size distribution and a fracture scenario that looks more like damage percolation [37]. As our previous findings indicate, this stabilizing effect is much more effective for mobile bonds, because mobility allows these bonds to accumulate near the crack tips. To verify this, we calculate the distribution of double bonds located on the surface of the cracks, $P(N_{b,2})$. As shown in Fig. 3(e), this distribution is initially similar for slip and catch bonds, but as the damage process proceeds and stresses increase, $P(N_{b,2})$ develops a much longer tail for the catch bonds. This shows that the increase in the number of double bonds observed in Fig. 2(d) is caused by an accumulation of catch bonds at the crack surface, where the local stress is highest. This accumulation of catch bonds in high stress regions is further confirmed by looking at the skewness of the bond length distribution $\hat{\mu}_3$, as shown in Fig. 3(f). In Figs. S8 and S9 in the Supplemental Material [33], we show that similar results are obtained at different stress values.

As discussed above, the fracture process appears to proceed differently for the two types of bonds. To investigate this in more detail, we calculate the fractal dimension d_f of the final percolating crack by using the box-counting method [38,39] (Figs. S13 and S14 in the Supplemental Material [33]). For immobile slip bonds, d_f depends weakly on the stress and has a value close to 1, which is the value expected for linear crack propagation, and corresponds to brittle fracture behavior [26,40]. For both immobile and mobile catch bonds, the fractal dimension is much larger than for the corresponding slip bonds, in particular at low stresses. This is in accordance with a scenario of damage percolation, and can also be seen by considering the total number of broken bonds at the moment of fracture, which is larger for catch bonds than for slip bonds (Figs. S4 and S12 in the Supplemental Material [33]). At higher stress, d_f decreases, indicating a transition to more brittle failure. This can be explained by the fact that at high forces the catch bonds return to slip behavior [Fig. 1(a)].

In conclusion, our results highlight how crosslinker dynamics affect the stability and fracture of transient networks. Many biological materials, such as the actin cytoskeleton, are crosslinked by dynamic and mobile linkers, probably because this allows for fast dynamic control of the network properties. Our simulations show

that for slip bonds, linker mobility seriously decreases the resistance of the networks to stress, while catch-bonded networks become more stable when the bonds are mobile. This suggests that mobile biological catch bonds have evolved as a strategy to realize flexibility and dynamics without compromising the resistance to mechanical stress. It should be possible to measure the differences in the spatial distribution of catch and slip bonds experimentally by using fluorescently labeled crosslinking proteins that can be tracked and localized using confocal or super-resolution microscopy [41]. By preparing networks with well-defined defects, this would allow one to validate our prediction that mobile slip bonds diffuse away from high-stress regions, while mobile catch bonds accumulate in these regions. In our simulations, we have considered two limiting cases, of completely immobile crosslinkers and of mobile crosslinkers that can diffuse throughout the whole network before rebinding. The actual distance that a crosslinker diffuses before rebinding can be estimated as $L_d \simeq \sqrt{Dt^b}$, where D is the diffusion coefficient and $t_b \simeq 1/k_0^b$ the rebinding time. When L_d is much smaller than the mesh size ξ of the network, the crosslinkers will rebind predominantly in the same region and can be considered immobile, while for $L_d \gg \xi$, the crosslinkers can diffuse away, corresponding to the mobile crosslinkers considered here. Hence, by varying the mesh size of the networks, it may be possible to observe a transition from the immobile to the mobile crosslinker scenario in experiments. Finally, we emphasize that we have focused here on networks that are crosslinked by either catch or slip bonds. However, most probably, cells use a combination of slip and catch bonds to tailor the mechanical response and dynamics at various stress levels. We hope that our results will help in understanding the complex dynamic behavior of biological networks, and inspire the design of novel synthetic materials with mechanical properties that cannot be realized with simple transient bonds.

This work is part of the SOFTBREAK project funded by the European Research Council (Consolidator grant Softbreak, Grant Agreement No. 682782). The authors acknowledge Simone Dussi, Frans Leermakers, and Martijn van Galen for useful discussions.

*Corresponding author.
jasper.vandergucht@wur.nl

[1] P. J. Skrzeszewska, J. Sprakel, F. A. de Wolf, R. Fokkink, M. A. Cohen Stuart, and J. van der Gucht, Fracture and self-healing in a well-defined self-assembled polymer network, Macromolecules **43**, 3542 (2010).
[2] O. Lieleg, K. Schmoller, M. M. A. E. Claessens, and A. R. Bausch, Cytoskeletal polymer networks: Viscoelastic properties are determined by the microscopic interaction potential of cross-links, Biophys. J. **96**, 4725 (2009).
[3] F. Huber, A. Boire, M. P. López, and G. H. Koenderink, Cytoskeletal crosstalk: When three different personalities team up, Curr. Opin. Cell Biol. **32**, 39 (2015).
[4] M. Mak, Impact of crosslink heterogeneity on extracellular matrix mechanics and remodeling, Comput. Struct. Biotechnol. J. **18**, 3969 (2020).
[5] K. Mayumi, J. Guo, T. Narita, C. Y. Hui, and C. Creton, Fracture of dual crosslink gels with permanent and transient crosslinks, Extreme Mech. Lett. **6**, 52 (2016).
[6] C. L. Lewis, K. Stewart, and M. Anthamatten, The influence of hydrogen bonding side-groups on viscoelastic behavior of linear and network polymers, Macromolecules **47**, 729 (2014).
[7] K. J. Henderson, T. C. Zhou, K. J. Otim, and K. R. Shull, Ionically cross-linked triblock copolymer hydrogels with high strength, Macromolecules **43**, 6193 (2010).
[8] M. Lemmers, J. Sprakel, I. Voets, J. van der Gucht, and M. Cohen Stuart, Multiresponsive reversible gels based on charge-driven assembly, Angew. Chem. **49**, 708 (2010).
[9] H. M. van der Kooij, S. Dussi, G. T. van de Kerkhof, R. A. Frijns, J. van der Gucht, and J. Sprakel, Laser speckle strain imaging reveals the origin of delayed fracture in a soft solid, Sci. Adv. **4**, eaar1926 (2018).
[10] B. T. Marshall, M. Long, J. W. Piper, T. Yago, R. P. McEver, and C. Zhu, Direct observation of catch bonds involving cell-adhesion molecules, Nature (London) **423**, 190 (2003).
[11] Z. Liu, H. Liu, A. M. Vera, R. C. Bernardi, P. Tinnefeld, and M. A. Nash, High force catch bond mechanism of bacterial adhesion in the human gut, Nat. Commun. **11**, 1 (2020).
[12] B. Liu, W. Chen, B. D. Evavold, and C. Zhu, Accumulation of dynamic catch bonds between tcr and agonist peptide-mhc triggers t cell signaling, Cell **157**, 357 (2014).
[13] V. C. Luca, B. C. Kim, C. Ge, S. Kakuda, D. Wu, M. Roein-Peikar, R. S. Haltiwanger, C. Zhu, T. Ha, and K. C. Garcia, Notch-jagged complex structure implicates a catch bond in tuning ligand sensitivity, Science **355**, 1320 (2017).
[14] W. E. Thomas, E. Trintchina, M. Forero, V. Vogel, and E. V. Sokurenko, Bacterial adhesion to target cells enhanced by shear force, Cell **109**, 913 (2002).
[15] D. L. Huang, N. A. Bax, C. D. Buckley, W. I. Weis, and A. R. Dunn, Vinculin forms a directionally asymmetric catch bond with f-actin, Science **357**, 703 (2017).
[16] J. M. Laakso, J. H. Lewis, H. Shuman, and E. M. Ostap, Myosin i can act as a molecular force sensor, Science **321**, 133 (2008).
[17] N. Y. Yao, C. P. Broedersz, M. Depken, D. J. Becker, M. R. Pollak, F. C. MacKintosh, and D. A. Weitz, Stress-Enhanced Gelation: A Dynamic Nonlinearity of Elasticity, Phys. Rev. Lett. **110**, 018103 (2013).
[18] Y. Mulla, M. J. Avellaneda, A. Roland, L. Baldauf, S. J. Tans, and G. H. Koenderink, Weak catch bonds make strong networks, Nat. Mater. **21**, 1019 (2022).
[19] B. L. Doss, M. Pan, M. Gupta, G. Grenci, R.-M. Mège, C. T. Lim, M. P. Sheetz, R. Voituriez, and B. Ladoux, Cell response to substrate rigidity is regulated by active and passive cytoskeletal stress, Proc. Natl. Acad. Sci. U.S.A. **117**, 12817 (2020).
[20] Y. Mulla and G. H. Koenderink, Crosslinker mobility weakens transient polymer networks, Phys. Rev. E **98**, 062503 (2018).

[21] R. C. Arevalo, P. Kumar, J. S. Urbach, and D. L. Blair, Stress heterogeneities in sheared type-I collagen networks revealed by boundary stress microscopy, PLoS One **10**, e0118021 (2015).
[22] L. Liang, C. Jones, S. Chen, B. Sun, and Y. Jiao, Heterogeneous force network in 3d cellularized collagen networks, Phys. Biol. **13**, 066001 (2016).
[23] J. L. Shivers, J. Feng, A. Sharma, and F. C. MacKintosh, Normal stress anisotropy and marginal stability in athermal elastic networks, Soft Matter **15**, 1666 (2019).
[24] J. Ruiz-Franco and J. van Der Gucht, Force transmission in disordered fibre networks, Front. Cell Dev. Biol. **10** (2022).
[25] L. Zhang, D. Z. Rocklin, L. M. Sander, and X. Mao, Fiber networks below the isostatic point: Fracture without stress concentration, Phys. Rev. Mater. **1**, 052602(R) (2017).
[26] S. Dussi, J. Tauber, and J. Van Der Gucht, Athermal Fracture of Elastic Networks: How Rigidity Challenges the Unavoidable Size-Induced Brittleness, Phys. Rev. Lett. **124**, 018002 (2020).
[27] D. T. Gillespie, A general method for numerically simulating the stochastic time evolution of coupled chemical reactions, J. Comput. Phys. **22**, 403 (1976).
[28] G. Bell, Models for the specific adhesion of cells to cells, Science **200**, 618 (1978).
[29] Y. V. Pereverzev, O. V. Prezhdo, M. Forero, E. V. Sokurenko, and W. E. Thomas, The two-pathway model for the catch-slip transition in biological adhesion, Biophys. J. **89**, 1446 (2005).
[30] M. van Galen, J. van der Gucht, and J. Sprakel, Chemical design model for emergent synthetic catch bonds, Front. Phys. **8** (2020).
[31] E. Bitzek, P. Koskinen, F. Gähler, M. Moseler, and P. Gumbsch, Structural Relaxation Made Simple, Phys. Rev. Lett. **97**, 170201 (2006).
[32] C. P. Broedersz and F. MacKintosh, Modeling semiflexible polymer networks, Rev. Mod. Phys. **86**, 955 (2016).
[33] See Supplemental Material http://link.aps.org/supplemental/10.1103/PhysRevLett.130.118203 for details on simulation methods and additional results.
[34] N. Y. Yao, D. J. Becker, C. P. Broedersz, M. Depken, F. C. MacKintosh, M. R. Pollak, and D. A. Weitz, Nonlinear viscoelasticity of actin transiently cross-linked with mutant α-actinin-4, J. Mol. Biol. **411**, 1062 (2011).
[35] F. Sciortino, P. Tartaglia, and E. Zaccarelli, One-dimensional cluster growth and branching gels in colloidal systems with short-range depletion attraction and screened electrostatic repulsion, J. Phys. Chem. B **109**, 21942 (2005).
[36] C. Inglis, Stresses in plates due to the presence of cracks and sharp corners, Trans. Inst. Nav. Archit. **55**, 219 (1913).
[37] A. Shekhawat, S. Zapperi, and J. P. Sethna, From Damage Percolation to Crack Nucleation Through Finite Size Criticality, Phys. Rev. Lett. **110**, 185505 (2013).
[38] J. Gagnepain and C. Roques-Carmes, Fractal approach to two-dimensional and three-dimensional surface roughness, Wear **109**, 119 (1986).
[39] J. Ruiz-Franco, F. Camerin, N. Gnan, and E. Zaccarelli, Tuning the rheological behavior of colloidal gels through competing interactions, Phys. Rev. Mater. **4**, 045601 (2020).
[40] A. A. Moreira, C. L. N. Oliveira, A. Hansen, N. A. M. Araújo, H. J. Herrmann, and J. S. Andrade Jr, Fracturing Highly Disordered Materials, Phys. Rev. Lett. **109**, 255701 (2012).
[41] R. Riera, T. Hogervorst, W. Doelman, Y. Ni, S. Pujals, E. Bolli, J. Codee, van Kasteren S. I., and L. Albertazzi, Single-molecule imaging of glycan-lectin interactions on cells with glyco-paint, Nat. Chem. Biol. **17**, 1281 (2021).